Real-Time Energy Management in Microgrids

Wenbo Shi, *Student Member, IEEE*, Na Li, *Member, IEEE*, Chi-Cheng Chu, and Rajit Gadh

***Abstract*—Energy management in microgrids is typically formulated as an offline optimization problem for day-ahead scheduling by previous studies. Most of these offline approaches assume perfect forecasting of the renewables, the demands, and the market, which is difficult to achieve in practice. Existing online algorithms, on the other hand, oversimplify the microgrid model by only considering the aggregate supply-demand balance while omitting the underlying power distribution network and the associated power flow and system operational constraints. Consequently, such approaches may result in control decisions that violate the real-world constraints. This paper focuses on developing an online energy management strategy (EMS) for real-time operation of microgrids that takes into account the power flow and system operational constraints on a distribution network. We model the online energy management as a stochastic optimal power flow problem and propose an online EMS based on Lyapunov optimization. The proposed online EMS is subsequently applied to a real-microgrid system. The simulation results demonstrate that the performance of the proposed EMS exceeds a greedy algorithm and is close to an optimal offline algorithm. Lastly, the effect of the underlying network structure on energy management is observed and analyzed.**

***Index Terms*—Distribution networks, energy management, Lyapunov optimization, microgrids, online algorithms, optimal power flow (OPF), real time.**

I. Introduction

A MICROGRID is a low-voltage power distribution system integrated with distributed energy resources (DERs) and controllable loads, which can be operated with or without the main grid [1]. DERs include a variety of distributed generation (DG) units such as wind turbines (WTs) and photovoltaics (PVs) and distributed storage (DS) units such as batteries. Controllable loads such as heating, ventilation, and air conditioning (HVAC) systems and electric vehicles (EVs) can be shed or shifted to balance supply and demand in a microgrid. An energy management strategy (EMS) is required in a microgrid to control power flows in order to meet certain operational objectives (e.g., minimizing costs) by adjusting the power imported/exported from/to the main grid, the dispatchable DERs, and the controllable loads [1].

Manuscript received January 23, 2015; revised April 10, 2015 and June 16, 2015; accepted July 23, 2015. This work was supported by the Research and Development Program of the Korea Institute of Energy Research under Grant B4-2411-01. Paper no. TSG-00074-2015.

W. Shi, C.-C. Chu, and R. Gadh are with the Smart Grid Energy Research Center, University of California, Los Angeles, CA 90095 USA (e-mail: wenbos@ucla.edu; peterchu@ucla.edu; gadh@ucla.edu).

N. Li is with the Department of Electrical Engineering, Harvard University, Cambridge, MA 02138, USA (e-mail: nali@seas.harvard.edu).

Color versions of one or more of the figures in this paper are available online at http://ieeexplore.ieee.org.

Digital Object Identifier 10.1109/TSG.2015.2462294

Energy management in microgrids is typically formulated as an offline optimization problem for day-ahead scheduling by [2]–[6]. Most of these offline approaches assume perfect forecasting of the renewables, the demands, and the market, which is difficult to achieve in practice due to the intermittency and variability of renewables, the spatial and temporal uncertainty in controllable loads (e.g., EVs), and the randomness in real-time pricing. To tackle this problem, efforts have been made to capture the uncertainties in day-ahead scheduling through modeling different scenarios [7]–[12]. These approaches typically use stochastic programming to formulate energy management as a deterministic problem based on the scenarios that are usually generated by Monte Carlo simulations. The number of these scenarios may be large and thus it can be computationally expensive to use these methods. Although these approaches consider the uncertainties, they still require certain forecasting and usually do not adapt to real-time changes in the environment. Siano *et al.* [13] and Pourmousavi *et al.* [14] considered the energy management problem at each time independently and focus on how to efficiently solve the optimization problem in real time.

Recently, there have been attempts to develop online algorithms for real-time energy management in microgrids to optimize the long-term cost, which take into account the uncertainties of the renewables, the demands, and the market [15]–[17]. These approaches do not require any *a priori* statistical knowledge of the underlying stochastic processes and can adapt to the time-varying environment. However, these existing online approaches consider the aggregate supply-demand balance while omitting the underlying power distribution network, the associated power flow (e.g., Kirchhoffs laws), and system operational constraints (e.g., voltage tolerances). Consequently, such approaches may result in control decisions that violate the real-world constraints.

Therefore, this paper focuses on developing an online EMS for real-time operation of microgrids that takes into account the power flow and system operational constraints on a distribution network. The objective of the EMS is to control power flows in the microgrid using only the current system state information at each time in order to: 1) minimize the long-term operational cost, including the cost of generation, the cost of energy storage, the cost of load shedding, and the cost of energy purchase from the main grid; 2) guarantee the quality-of-service for customers; and 3) minimize the long-term power losses subject to the DER constraints, the load constraints, the power flow constraints, and the system operational constraints (e.g., voltage tolerances).

Specifically, we formulate the online energy management in microgrids as a stochastic optimal power flow (SOPF) problem. Although dynamic programming (DP) techniques

could be applied to solve the stochastic optimization problem, they would result in complex solutions that are time-consuming to compute, thus preventing them to be suitable for real-time applications.[1] Moreover, because DP methods usually require assumptions of the underlying stochastic processes, it is difficult for them to adapt to any changing probabilities or any un-modeled uncertainties in the actual processes [18]. Therefore, we adopt Lyapunov optimization [19] to design an online EMS that simply uses the current system state to achieve real-time energy management without any *a priori* statistical knowledge of the underlying stochastic processes. Lyapunov optimization is a technique for optimizing time averages in stochastic networks. It has been recently applied to various aspects of smart grid, e.g., home energy management [18], [20], demand response [21], electrical vehicle charging and vehicle-to-grid control [22], [23], energy storage management [24]–[26], and microgrid energy management [15]–[17]. Most of the studies on Lyapunov optimization consider an infinite-time horizon, which may cause issues under certain circumstances [26]. See [26] on how to optimize over a finite-time horizon under the Lyapunov framework.

To solve the SOPF problem, we first use the concept of virtual queues from Lyapunov optimization to obtain a relaxed SOPF problem (SOPF-r) to deal with the time-coupled constraints. We then reformulate SOPF-r as an optimal power flow problem (OPF) to be solved at each time using the drift-plus-penalty algorithm from Lyapunov optimization. OPF is NP-hard to solve in general due to the quadratic power flow constraints [27]. We therefore relax the constraints and obtain a convex optimization problem for real-time computing (see [27], [28] for a tutorial on convex relaxation of OPF). Sufficient conditions for the exactness of the relaxation have been derived in [29]–[31], which hold for a variety of IEEE test systems and real-world distribution systems. Our proposed online EMS uses only the current system state information to solve a convex OPF problem and thus is simple and efficient to implement in real time.

As one demonstration, we apply the proposed online EMS to a real-microgrid system in Guangdong Province, China. We evaluate the performance of the proposed online EMS with two benchmarks: 1) an optimal offline algorithm that solves the optimization problem over the entire time horizon assuming that all system states over time are known *a priori*; and 2) a greedy algorithm that optimizes the cost at each time independently. The simulation results show that the proposed online EMS outperforms the greedy algorithm and its performance is close to the optimal offline algorithm. Regarding real-time computing, the computational time of our proposed online EMS at each time step is on average 1.13 s showing that it can be implemented in real time.

In order to compare with previous online approaches [15]–[17], we also solve the microgrid energy management problem without considering the underlying network constraints and then compute the power flows based on the obtained control decisions. Our simulation results demonstrate that those online approaches can lead to bus voltages that violate the tolerance constraints significantly. In contrast, our proposed online EMS is able to achieve the long-term objective while maintaining the voltages within the tolerance. The simulation results also show the network effect that the loads behave differently based on their locations. Therefore, by incorporating the distribution network in the modeling, this paper presents the relationship between the physical structure of a microgrid and the online energy management on the network.

The rest of this paper is organized as follows. We introduce the system model in Section II and propose the online EMS in Section III. Simulation results are provided in Section IV and the conclusion is given in Section V.

[1]DP techniques generally suffer from the "curse-of-dimensionality" [18] which makes them difficult to apply to large systems due to the real-time computational requirement.

II. System Model

In this section, we describe the system model for developing the proposed online EMS. We first give an overview of the system followed by the DG model, the DS model, and the load model. We then model the power distribution network using a branch flow model and formulate real-time microgrid energy management as an SOPF problem.

A. System Overview

Consider a microgrid with a set of DG units denoted by $\mathcal{G} \triangleq \{g_1, g_2, \ldots, g_G\}$, DS units denoted by $\mathcal{B} \triangleq \{b_1, b_2, \ldots, b_B\}$, and controllable loads denoted by $\mathcal{L} \triangleq \{l_1, l_2, \ldots, l_L\}$. We assume the structure of the microgrid to be radial as most of the power distribution networks are radial [32]. All DER units and loads are connected by a two-way real-time communication infrastructure linking the microgrid central controller (MGCC) and the local controllers (LCs). The MGCC is able to gather real-time information from the LCs, perform energy management, and send control commands to the LCs. Fig. 1 shows the overall system architecture. In this paper, we use a discrete-time model, assuming that the system operates in discrete time with $t \in \{0, 1, 2, \ldots\}$ and time interval Δt.

B. DG Model

We consider two types of DG units in the microgrid: 1) nondispatchable renewable DG units denoted by $g \in \mathcal{G}_r$ such as PVs and WTs and 2) dispatchable conventional DG units denoted by $g \in \mathcal{G}_c$ such as diesel. For each DG $g \in \mathcal{G}$, we denote its complex output power by $s_g(t) \triangleq p_g(t) + \mathbf{i}q_g(t)$, where $p_g(t)$ is the active power and $q_g(t)$ is the reactive power.

1) Renewable DG: A renewable DG unit such as PV or WT is not dispatchable and its output power is dependent on the availability of the primary sources (i.e., sun irradiance or wind). Therefore, we assume $p_g(t)$ and $q_g(t)$ are both random variables due to the stochastic nature of renewable DGs and there is no generation cost. Note that we consider the renewable DG unit with an on-site battery storage system as two separate units. Such a system can be modeled as a nondispatchable DG unit and a DS unit at the same bus.

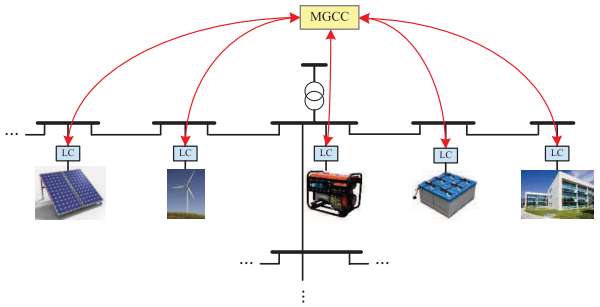

Fig. 1. System architecture [6].

2) Conventional DG: A conventional DG unit such as diesel is a dispatchable source, its output power is a variable with the following constraints: $\forall g \in \mathcal{G}_c, t$:

$$0 \le p_g(t) \le \bar{p}_g \tag{1}$$

$$|p_g(t) - p_g(t-1)| \le r_g \bar{p}_g \tag{2}$$

where $\bar{p}_g$ is the maximum output power and $r_g \in (0, 1]$ is the ramping parameter.

The reactive power generated at the inverter is bounded by

$$p_g(t)^2 + q_g(t)^2 \le s_g^2, \ \ \forall g \in \mathcal{G}_c, t \tag{3}$$

where s_g is the capacity of the inverter.

We model the conventional DG generation cost at each time t using a quadratic model [7]

$$C_g(p_g(t)) \triangleq \alpha_g \big(p_g(t)\Delta t\big)^2 + \beta_g p_g(t)\Delta t + c_g \tag{4}$$

where α_g, β_g, and c_g are constants.

C. DS Model

We consider batteries as the DS units in the microgrid. For a given battery $b \in \mathcal{B}$, we denote its complex power by $s_b(t) \triangleq p_b(t) + \mathbf{i}q_b(t)$, where $p_b(t)$ is the active power (positive when charging and negative when discharging) and $q_b(t)$ is the reactive power. Let $E_b(t)$ denote the energy stored in the battery at time t. A given battery $b \in \mathcal{B}$ can be modeled by the following constraints: $\forall t$:

$$\underline{p}_b \le p_b(t) \le \bar{p}_b \tag{5}$$

$$p_b(t)^2 + q_b(t)^2 \le s_b^2 \tag{6}$$

$$E_b(t+1) = E_b(t) + p_b(t)\Delta t \tag{7}$$

$$\underline{E}_b \le E_b(t) \le \bar{E}_b \tag{8}$$

where $\bar{p}_b$ is the maximum charging rate, $-\underline{p}_b$ is the maximum discharging rate, s_b is the capacity of the inverter, and $\underline{E}_b$ and $\bar{E}_b$ are the minimum and maximum allowed energy stored in the battery, respectively.

We model the cost of operating a given battery b at each time t as [17]

$$C_b(p_b(t)) \triangleq \alpha_b p_b(t)^2 + c_b \tag{9}$$

where α_b and c_b are constants. The cost function penalizes fast charging/discharing which is harmful to battery life.

D. Load Model

We consider a demand side management (DSM) in the microgrid, where flexible loads such as HVAC and EVs, and smart appliances can be shed in response to supply conditions. For each load $l \in \mathcal{L}$, we denote its complex power by $s_l(t) \triangleq p_l(t) + \mathbf{i}q_l(t)$ and it is bounded by: $\forall t$

$$\underline{p}_l(t) \le p_l(t) \le \bar{p}_l(t) \tag{10}$$

$$\underline{q}_l(t) \le q_l(t) \le \bar{q}_l(t) \tag{11}$$

where $\underline{p}_l(t)$ is the minimum power required by the load that cannot be shed, $\bar{p}_l(t)$ is the maximum power requested by the load, and $\underline{q}_l(t)$ and $\bar{q}_l(t)$ are the minimum and maximum reactive power. $\underline{p}_l(t)$, $\bar{p}_l(t)$, $\underline{q}_l(t)$, and $\bar{q}_l(t)$ are the demand request generated by customers based on the physical constraints and their willingness to participate in the DSM. If a customer refuses load shedding, the requested maximum and minimum power will be the same giving no flexility for the EMS. On the EMS side, the demand requests are assumed to stochastic and unknown, and they are provided by the customers at each time. Customers may use an intelligent algorithm to generate their requests. One direction for future work is to design such an algorithm on the customer side.

In order to control the quality-of-service [16] for customers in the microgrid, we impose an upper bound on the time average load shedding percentage [17]

$$\lim_{T\to\infty} \frac{1}{T} \sum_{t=0}^{T-1} \mathbb{E}\left[\frac{\bar{p}_l(t) - p_l(t)}{\bar{p}_l(t) - \underline{p}_l(t)}\right] \le \alpha_l, \ \ \forall l \tag{12}$$

where $\bar{p}_l(t) - \underline{p}_l(t)$ is the total demand that can be shed, $\bar{p}_l(t) - p_l(t)$ is the shed demand, and α_l is a positive constant to control the quality-of-service. A small α_l means tighter quality-of-service control.

We use a cost function to capture the cost of load shedding in the DSM

$$C_l(t, p_l(t)) \triangleq \beta_l(\bar{p}_l(t)\Delta t - p_l(t)\Delta t)^2 \tag{13}$$

where β_l is a positive constant. α_l and β_l reflect the customer's tolerance and sensitivity to load shedding and they are assumed to be generated on the customer side.

Note that although both (12) and (13) can limit load shedding to some extent, they have different meanings in the model. While (13) captures the economic loss of load shedding in the objective of the EMS, (12) is a constraint to guarantee the quality-of-service in a time-average sense that can be seen as a "soft" limit on load shedding.

E. Distribution Network Model

A distribution network is composed of lines and buses. It can be modeled as a connected graph $(\mathcal{N}, \mathcal{E})$, where each node $i \in \mathcal{N}$ represents a bus and each link $(i, j) \in \mathcal{E}$ represents a branch (line or transformer). A power distribution network typically has a radial structure and the graph becomes a tree. The root of the tree is the feeder with a fixed voltage and flexible power injection, denoted by bus 0. We index the other buses in $\mathcal{N}$ by $i = 1, \ldots, n$.

For each link $(i,j) \in \mathcal{E}$, let $z_{ij} \triangleq r_{ij} + \mathbf{i}x_{i,j}$ be the complex impedance of the branch, $I_{ij}(t)$ be the complex current from buses i to j, and $S_{ij}(t) \triangleq P_{ij}(t) + \mathbf{i}Q_{ij}(t)$ be the complex power flowing from buses i to j.

For each bus $i \in \mathcal{N}$, let $V_i(t)$ be the complex voltage at bus i and $s_i(t) \triangleq p_i(t) + \mathbf{i}q_i(t)$ be the net load which is the load minus the generation at bus i. Each bus $i \in \mathcal{N} \setminus \{0\}$ is connected to a subset of DG units $\mathcal{G}_i$, DS units $\mathcal{B}_i$, and loads $\mathcal{L}_i$. The net load at each bus i satisfies

$$s_i(t) = s_{li}(t) + s_{bi}(t) - s_{gi}(t), \ \forall i \in \mathcal{N} \setminus \{0\}, t \tag{14}$$

where $s_{li}(t) \triangleq \sum_{l \in \mathcal{L}_i} s_l(t)$, $s_{bi}(t) \triangleq \sum_{b \in \mathcal{B}_i} s_b(t)$, and $s_{gi} \triangleq \sum_{g \in \mathcal{G}_i} s_g(t)$.

The steady-state power flows in a given distribution network $(\mathcal{N}, \mathcal{E})$ can be modeled using the branch flow model [27]: $\forall (i,j) \in \mathcal{E}, t$

$$p_j(t) = P_{ij}(t) - r_{ij}\ell_{ij}(t) - \sum_{k:(j,k)\in\mathcal{E}} P_{jk}(t) \tag{15}$$

$$q_j(t) = Q_{ij}(t) - x_{ij}\ell_{ij}(t) - \sum_{k:(j,k)\in\mathcal{E}} Q_{jk}(t) \tag{16}$$

$$v_j(t) = v_i(t) - 2\big(r_{ij}P_{ij}(t) + x_{ij}Q_{ij}(t)\big) + \Big(r_{ij}^2 + x_{ij}^2\Big)\ell_{ij}(t) \tag{17}$$

$$\ell_{ij}(t) = \frac{P_{ij}(t)^2 + Q_{ij}(t)^2}{v_i(t)} \tag{18}$$

where $\ell_{ij}(t) \triangleq |I_{ij}(t)|^2$ and $v_i(t) \triangleq |V_i(t)|^2$.

Equations (15)–(18) define a system of equations in the variables $(\mathbf{P}(t), \mathbf{Q}(t), \mathbf{v}(t), \mathbf{l}(t), \mathbf{s}(t))$, where $\mathbf{P}(t) \triangleq (P_{ij}(t), (i,j) \in \mathcal{E})$, $\mathbf{Q}(t) \triangleq (Q_{ij}(t), (i,j) \in \mathcal{E})$, $\mathbf{v}(t) \triangleq (v_i(t), i \in \mathcal{N} \setminus \{0\})$, $\mathbf{l}(t) \triangleq (\ell_{ij}(t), (i,j) \in \mathcal{E})$, and $\mathbf{s}(t) \triangleq (s_i(t), i \in \mathcal{N} \setminus \{0\})$. The phase angles of the voltages and the currents are not included. But they can be uniquely determined for radial systems [28].

F. Real-Time Energy Management

The objective of the microgrid operator is to minimize its long-term operational cost, while delivering reliable and high-quality power to the customers. However, the introduction of DERs brings uncertainties to the energy management problem, which makes it challenging to balance supply and demand in real time. The voltages in the microgrid may also deviate significantly from the nominal values. Thus, in this paper, we study microgrid energy management aiming at achieving the long-term operational objective of the microgrid operator, while meeting the supply-demand balance and the voltage tolerance constraints in real time.

We consider the following voltage tolerance constraints in the microgrid:

$$\underline{V}_i \le |V_i(t)| \le \bar{V}_i, \ \forall i \in \mathcal{N} \setminus \{0\}, t \tag{19}$$

where $\underline{V}_i$ and $\bar{V}_i$ correspond to the minimum and maximum allowed voltages, respectively.

The net power injected to the microgrid from the main grid is given by

$$s_0(t) = \sum_{j:(0,j)\in\mathcal{E}} s_{0j}(t), \ \forall t. \tag{20}$$

If the microgrid is operated in islanded mode, then $s_0(t) = 0$. If the microgrid is operated in grid-connected mode, then $s_0(t)$ is the net complex power traded between the microgrid and the main grid. We model the cost of energy purchase from the main grid at each time t as

$$C_0(t, p_0(t)) \triangleq \rho(t) p_0(t) \Delta t \tag{21}$$

where $\rho(t)$ is the market energy price. Note that $p_0(t)$ can be negative, meaning that the microgrid can sell its surplus power to the main grid.

We define the system state vector at time t using the renewable generations, the demand requests, and the energy price

$$\mathbf{x}(t) \triangleq (\mathbf{r}(t), \mathbf{d}(t), \rho(t)) \tag{22}$$

where $\mathbf{r}(t) \triangleq (s_g(t), g \in \mathcal{G}_r)$ is the vector of renewable generations and $\mathbf{d}(t) \triangleq (\underline{p}_l(t), \bar{p}_l(t), \underline{q}_l(t), \bar{q}_l(t), l \in \mathcal{L})$ is the vector of demand requests. We assume the system state to be stochastic and make no assumptions about the statistics of the underlying stochastic processes.

We define the control vector at time t as

$$\mathbf{u}(t) \triangleq (\mathbf{P}(t), \mathbf{Q}(t), \mathbf{v}(t), \mathbf{l}(t), \mathbf{s}(t), \mathbf{g}(t), \mathbf{b}(t), \mathbf{y}(t)) \tag{23}$$

where $\mathbf{g}(t) \triangleq (s_g(t), g \in \mathcal{G}_c)$, $\mathbf{b}(t) \triangleq (s_b(t), b \in \mathcal{B})$, and $\mathbf{y}(t) \triangleq (s_l(t), l \in \mathcal{L})$. $\mathbf{u}(t)$ controls power flows in the microgrid.

The objective of the real-time energy management in the microgrid is to make control decision $\mathbf{u}(t)$ at each time in order to: 1) minimize the long-term operational cost, including the cost of generation, the cost of energy storage, the cost of load shedding, and the cost of energy purchase from the main grid; 2) guarantee the quality-of-service for customers; and 3) minimize the long-term power losses subject to the DER constraints, the load constraints, the power flow constraints, and the system operational constraints (voltage tolerances).

We define the objective function of the optimization as

$$\begin{aligned} C(t) \triangleq \xi_g \sum_{g\in\mathcal{G}_c} C_g\big(p_g(t)\big) + \xi_b \sum_{b\in\mathcal{B}} C_b(p_b(t)) + \xi_l \sum_{l\in\mathcal{L}} C_l(t, p_l(t)) \\ + \xi_0 C_0(t, p_0(t)) + \xi_p \sum_{(i,j)\in\mathcal{E}} r_{ij}\ell_{ij}(t) \end{aligned} \tag{24}$$

where ξ_g, ξ_b, ξ_l, ξ_0, and ξ_p are the parameters to tradeoff among different costs and power losses in the optimization.

The real-time energy management in the microgrid can be formulated as an SOPF problem.

SOPF:

$$\begin{aligned} \min_{\{\mathbf{u}(t)\}} \quad & \lim_{T\to\infty} \frac{1}{T} \sum_{t=0}^{T-1} \mathbb{E}[C(t)] \\ \text{s.t.} \quad & (1)\text{–}(3), \ (5)\text{–}(8), \text{ and } (10)\text{–}(20) \end{aligned}$$

where the randomness of the system state $\mathbf{x}(t)$ and the possibly random control decision $\mathbf{u}(t)$ at each time are taken into account in the expectations in the objective and constraint (12).

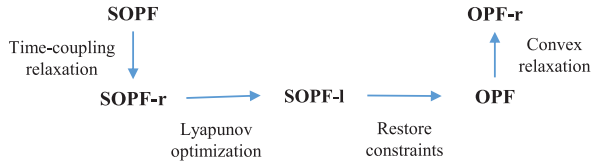

Fig. 2. Problem formulation scheme.

III. Online EMS

Solving the previous SOPF problem is challenging mainly due to the objective and constraints (8) and (12). We first use the concept of virtual queues from Lyapunov optimization (see [19, Sec. 4.4]) to deal with these constraints and obtain a relaxed SOPF problem (SOPF-r). Following the Lyapunov optimization framework (see Appendix A for a brief introduction or [19, Ch. 4] for details), we reformulate SOPF-r as a real-time problem (SOPF-l). Since we relax the constraints, the solution to SOPF-l may be infeasible to the original SOPF problem. Therefore, we restore the constraints and obtain a standard OPF problem to be solved at each time. The OPF problem is nonconvex due to the quadratic equality constraints in (18) and thus is NP-hard to solve in general [27]. We therefore relax the constraints and obtain a convex optimization problem (OPF-r) for real-time computing. Fig. 2 summarizes the scheme used in the problem formulation.

A. Virtual Queue Design

To deal with constraints (8) and (12), we use the concept of virtual queues (see [19, Sec. 4.4]) to help satisfy the constraints.

1) Battery Queue: We define a virtual queue $J_b(t)$ for each $b \in \mathcal{B}$ that accumulates the charging/discharging energy. Define $J_b(0) = 0$ and it updates as follows:

$$J_b(t+1) = J_b(t) + p_b(t)\Delta t, \ \ \forall t, b. \tag{25}$$

We define $\mathbf{J}(t) \triangleq (J_b(t), b \in \mathcal{B})$.

$J_b(t)$ is in fact a shifted version of the energy stored in the battery $E_b(t)$. Instead of requiring that $E_b(t)$ is always bounded by (8), we relax it to keep the battery queue $J_b(t)$ mean rate stable

$$\lim_{t\to\infty} \frac{\mathbb{E}[|J_b(t)|]}{t} = 0, \ \ \forall b. \tag{26}$$

2) Load Queue: We define a virtual queue $H_l(t)$ for each load $l \in \mathcal{L}$ to tackle the time average constraint in (12). Define $H_l(0) = 0$ and its backlog evolves as follows [19]:

$$H_l(t+1) = \max\{H_l(t) - \alpha_l, 0\} + \frac{\bar{p}_l(t) - p_l(t)}{\bar{p}_l(t) - \underline{p}_l(t)}, \ \ \forall t, l. \tag{27}$$

We define $\mathbf{H}(t) \triangleq (H_l(t), l \in \mathcal{L})$.

The arrival rate of the load queue $H_l(t)$ is the shedding percentage at time t and the departure rate is α_l. If the queue $H_l(t)$ is stable, the time average load shedding percentage must be less than or equal to α_l. Therefore, constraint (12) can be transformed to the following queue stability constraint [19]:

$$\lim_{t\to\infty} \frac{\mathbb{E}[|H_l(t)|]}{t} = 0, \ \ \forall l. \tag{28}$$

Now, we consider a relaxed SOPF problem that fits the Lyapunov optimization framework.

SOPF-r:

$$\begin{aligned} \min_{\{\mathbf{u}(t)\}} \quad & \lim_{T\to\infty} \frac{1}{T} \sum_{t=0}^{T-1} \mathbb{E}[C(t)] \\ \text{s.t.} \quad & (1),\ (3),\ (5)\text{–}(7),\ (10),\ (11) \\ & (14)\text{–}(20), \text{and } (25)\text{–}(28). \end{aligned}$$

Note the time-coupled generation ramping constraint (2) is also relaxed here. SOPF-r provides a lower bound on SOPF. If the optimal solution to SOPF-r is feasible to SOPF, then it is also an optimal solution to SOPF.

B. Lyapunov Optimization

It is still difficult to solve SOPF-r because of the objective function and constraints (26) and (28). To address these challenges, we follow the Lyapunov optimization framework (see Appendix A for a brief introduction or [19, Ch. 4] for details) to solve the above SOPF-r problem.

Define $\mathbf{\Theta}(t) \triangleq (\mathbf{J}(t), \mathbf{H}(t))$ and the Lyapnuov function as a scalar measure of $\mathbf{\Theta}(t)$

$$L(\mathbf{\Theta}(t)) \triangleq \frac{1}{2}\beta \sum_{b\in\mathcal{B}} J_b(t)^2 + \frac{1}{2} \sum_{l\in\mathcal{L}} H_l(t)^2 \tag{29}$$

where β is a weight to treat the battery virtual queue differently from the load virtual queue.

We define the conditional one-slot Lyapunov drift as follows:

$$\Delta(\mathbf{\Theta}(t)) \triangleq \mathbb{E}[L(\mathbf{\Theta}(t+1)) - L(\mathbf{\Theta}(t))|\mathbf{\Theta}(t)]. \tag{30}$$

The Lyapunov drift measures the expected queue size growth given the current state $\mathbf{\Theta}(t)$.

Minimizing the Lyapunov drift would push the queues toward a less congested state, but it may incur a high cost. Therefore, we minimize a weighted sum of the drift and cost, which is defined as a drift-plus-penalty function $\Delta(\mathbf{\Theta}(t)) + V\mathbb{E}[C(t)|\mathbf{\Theta}(t)]$, where V is a positive parameter to tradeoff between stabilizing queues and minimizing cost.

Lemma 1: For any possible control policies, the drift-plus-penalty function is upper bounded at each time t

$$\begin{aligned} \Delta(\mathbf{\Theta}(t)) + V\mathbb{E}[C(t)|\mathbf{\Theta}(t)] \le B + \beta \sum_{b\in\mathcal{B}} J_b(t)\mathbb{E}\big[p_b(t)\Delta t|\mathbf{\Theta}(t)\big] \\ + \sum_{l\in\mathcal{L}} H_l(t)\mathbb{E}\left[\frac{\bar{p}_l(t) - p_l(t)}{\bar{p}_l(t) - \underline{p}_l(t)} - \alpha_l|\mathbf{\Theta}(t)\right] + V\mathbb{E}[C(t)|\mathbf{\Theta}(t)] \end{aligned} \tag{31}$$

where $B \triangleq (1/2)\sum_{l\in\mathcal{L}}(1 + \alpha_l^2) + (1/2)\beta\sum_{b\in\mathcal{B}} \max\{\underline{p}_b^2, \bar{p}_b^2\}\Delta t^2$.

Proof: See Appendix B. ∎

Instead of minimizing the drift-plus-penalty function directly, we minimize the upper bound in (31) via the framework of opportunistically minimizing an expectation (see [19, Sec. 1.8]). The resulting algorithm can be described as follows. At each time t, observe the system state $\mathbf{x}(t)$ and the virtual queue states $\mathbf{\Theta}(t)$, and determine the control decision $\mathbf{u}(t)$ by solving the following optimization problem.

SOPF-l:

$$\begin{aligned}\min_{\mathbf{u}(t)} \quad & \beta \sum_{b\in\mathcal{B}} J_b(t)p_b(t)\Delta t - \sum_{l\in\mathcal{L}} \frac{H_l(t)}{\bar{p}_l(t)-\underline{p}_l(t)} p_l(t) + VC(t) \\ \text{s.t.} \quad & (1),\ (3),\ (5)\text{–}(7),\ (10),\ (11) \\ & (14)\text{–}(20),\ (25), \text{and } (27).\end{aligned}$$

The above algorithm does not require any information of the probabilities associated with the system state $\mathbf{x}(t)$. The queue states $\mathbf{\Theta}(t)$ carry sufficient statistical information needed to determine the control decision at the next time step.

Since we relax the generation ramping constraint (2) and the battery energy constraint (8) in SOPF-l, the optimal solution to SOPF-l may violate these constraints and thus may be infeasible to the original SOPF problem. Therefore, we add constraints (2) and (8) back. The problem we consider now is indeed a standard OPF problem to be solved at each time t.

OPF:

$$\begin{aligned}\min_{\mathbf{u}(t)} \quad & \beta \sum_{b\in\mathcal{B}} J_b(t)p_b(t)\Delta t - \sum_{l\in\mathcal{L}} \frac{H_l(t)}{\bar{p}_l(t)-\underline{p}_l(t)} p_l(t) + VC(t) \\ \text{s.t.} \quad & (1)\text{–}(3),\ (5)\text{–}(8),\ (10),\ (11) \\ & (14)\text{–}(20),\ (25), \text{and } (27).\end{aligned}$$

The solution to OPF is always feasible to SOPF.

C. Convexification of OPF

The previous OPF problem is nonconvex due to the quadratic equality constraint in (18) and is NP-hard to solve in general [27]. We therefore relax them to inequalities

$$\ell_{ij}(t) \geq \frac{P_{ij}(t)^2 + Q_{ij}(t)^2}{v_i(t)},\ \forall (i,j)\in\mathcal{E}, t. \tag{32}$$

We then consider the following convex relaxation of OPF.

OPF-r:

$$\begin{aligned}\min_{\mathbf{u}(t)} \quad & \beta \sum_{b\in\mathcal{B}} J_b(t)p_b(t)\Delta t - \sum_{l\in\mathcal{L}} \frac{H_l(t)}{\bar{p}_l(t)-\underline{p}_l(t)} p_l(t) + VC(t) \\ \text{s.t.} \quad & (1)\text{–}(3),\ (5)\text{–}(8),\ (10),\ (11),\ (14)\text{–}(17) \\ & (19)\text{–}(20),\ (25),\ (27), \text{and } (32).\end{aligned}$$

The above relaxation is exact if the solution to OPF-r is also an optimal solution to OPF, i.e., the equality in (32) is attained. In general, such a relaxation is not exact. It has been shown recently [29]–[31] that the convex relaxation of OPF is exact under certain mild conditions that can be checked *a priori*. Such conditions are verified to hold in a variety of IEEE test distribution systems and real-world distribution systems. Roughly speaking, the relaxation is exact if the power injection at each bus is not too large and the voltages are kept around their nominal values [33]. In this paper, we assume that the sufficient conditions specified in [31] hold for the microgrid and thus we focus on solving the OPF-r problem. The exactness of the relaxation is also verified numerically in the simulation. OPF-r is a convex optimization problem and therefore can be solved efficiently for real-time computation.

D. Performance Gaps in the Optimizations

From the Lyapunov optimization theory, it can be proved that the optimal time average cost of SOPF-l is within $O(1/V)$ of the optimal time average cost of SOPF-r, i.e., SOPF-l* $\leq$ SOPF-r*$+B/V$, with a corresponding $O(V)$ tradeoff in the average queue size with independent identically distributed (i.i.d.) system state (see [19, Th. 4.8]), and the algorithm is robust to non-i.i.d., nonergodic situations (see [19, Th. 4.13]). Since SOPF-r provides a lower bound on SOPF, i.e., SOPF-r* $\leq$ SOPF*, we obtain a deterministic performance bound on SOPF-l as SOPF-l* $\leq$ SOPF*$+B/V$. The choice of the control parameter V affects the performance of the optimization. A large V can decrease optimality gap but also increase the average queue size. On the other hand, a small V makes it easier to keep the queues stable but at the sacrifice of a larger optimality gap.

If the solution to OPF is the same as the solution to SOPF-l, the performance of the proposed online EMS can be guaranteed using the above performance bound. However, as we restore the constraints in OPF, it is possible that these constraints are effective in the optimal solution and thus affect the optimality. The previous studies [15]–[17] deal with this issue by carefully designing the control parameters to force the time-coupled constraints to be always satisfied in the solution to the Lyapunov optimization. Unfortunately, the same method cannot be applied here due to the difficulty in characterizing the solution brought up by the introduction of the power flow and system operational constraints. We therefore validate the performance of the proposed online EMS via simulations. Our simulation results in the next section will demonstrate that the performance of the proposed EMS is desirable.

IV. Performance Evaluation

In this section, we demonstrate the proposed online EMS by applying it to a real-microgrid system. We first describe the microgrid system and the simulation setup. We then describe two benchmarks and compare the proposed online EMS with them. Finally, we discuss the battery queue and the load queue behaviors, the voltages in the microgrid, and the network effect observed in the simulations.

A. Simulation Setup

Fig. 3 shows the configuration of a real-microgrid system [6] in Guangdong Province, China, consisting of PVs, WTs, diesel generators, and a battery energy storage system (BESS). The numbers under the DERs and the loads in the figure correspond to the maximum power. We use this microgrid to demonstrate the proposed online EMS. In the simulation, we run the proposed online EMS for four days denoted by $\mathcal{T} \triangleq \{0, 1, \ldots, T-1\}$. The time interval Δt in the model is 5 min and there are $T = 1152$ time intervals in total.

Fig. 4 shows the renewable generation profiles, the load profile, and the market prices used in the simulation. We use the real solar and wind data from national renewable energy laboratory [34] to generate the renewable generation profiles. For each load, we generate the maximum power request $\bar{p}_l(t)$ based on different types of load using a Gaussian random variable

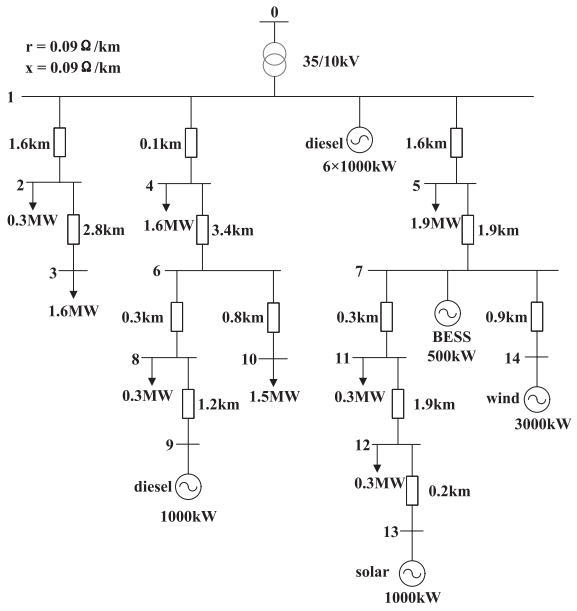

Fig. 3. Topology of the microgrid [6].

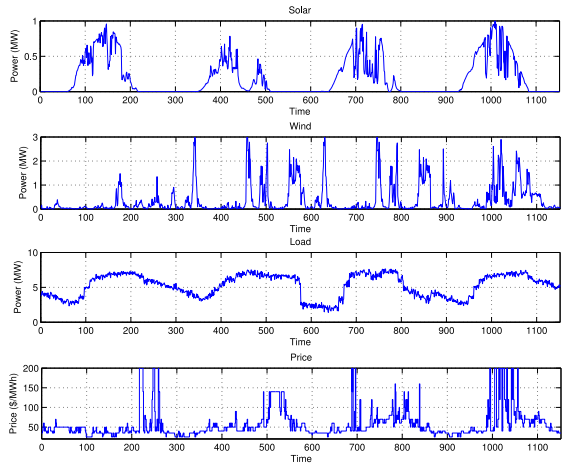

Fig. 4. Renewable generation profiles, load profile, and real-time price.

with hourly mean values from [6] and choose the percentage of load that can be shed $(\bar{p}_l(t) - \underline{p}_l(t)/\bar{p}_l(t))$ randomly from $[30\%, 50\%]$. The reactive power requests $\bar{q}_l(t)$ and $\underline{q}_l(t)$ are generated based on the active power requests $\bar{p}_l(t)$ and $\underline{p}_l(t)$ using a power factor chosen randomly from $[0.8, 0.9]$. The parameters α_l and β_l are chosen to be 0.5 and 500, respectively for each load. We use the 5-min real-time pricing data from CAISO [35] in the simulation. We set the cost function of diesel generation as $C_g(p_g(t)) \triangleq 40(p_g(t)\Delta t)^2 + 60(p_g(t)\Delta t)$ and the ramping parameter as $r_g = 0.3$. The capacity of the BESS $\bar{E}_b$ is 3 MWh and $\underline{E}_b$ is chosen to be 0.1 MWh. The initial battery energy level is set to be $E_b(0) = 1.5$ MWh. The parameters in the battery cost function are chosen as $\alpha_b = 1$ and $c_b = 0$.

B. Benchmarks

In order to evaluate the performance of the proposed online EMS, we use two benchmarks: 1) an optimal offline algorithm that optimizes the objective over the entire time horizon $\mathcal{T}$; and 2) a greedy algorithm that optimizes the cost at each time independently.

The offline algorithm solves the following optimization problem over the entire time horizon $\mathcal{T}$.

Offline:

$$\begin{aligned} \min_{\{\mathbf{u}(t)\}} \quad & \frac{1}{T}\sum_{t=0}^{T-1} C(t) \\ \text{s.t.} \quad & (1)\text{–}(3),\ (5)\text{–}(8),\ (10),\ (11), \text{and } (14)\text{–}(20) \\ & \frac{1}{T}\sum_{t=0}^{T-1} \frac{\bar{p}_l(t) - p_l(t)}{\bar{p}_l(t) - \underline{p}_l(t)} \le \alpha_l,\ \forall l. \end{aligned}$$

The offline algorithm provides a lower bound on any online algorithms, assuming that all system states over time (i.e., the output power of the renewables, the demand requests, and the energy prices) are known *a priori*, which is difficult to achieve in practice due to the stochastic nature of the problem. Although the optimal solution to the offline problem is not achievable in practice, it gives us the best performance to compare with any online algorithms.

Another benchmark we consider is a greedy algorithm that aims to minimize the cost at each time $t \in \mathcal{T}$ independently.

Greedy:

$$\begin{aligned} \min_{\mathbf{u}(t)} \quad & C(t) \\ \text{s.t.} \quad & (1)\text{–}(3),\ (5)\text{–}(8),\ (10),\ (11),\ (14)\text{–}(20) \\ & \frac{\bar{p}_l(t) - p_l(t)}{\bar{p}_l(t) - \underline{p}_l(t)} \le \alpha_l,\ \forall l. \end{aligned}$$

The greedy algorithm is shortsighted as it optimizes the cost at each time without taking the future into account.

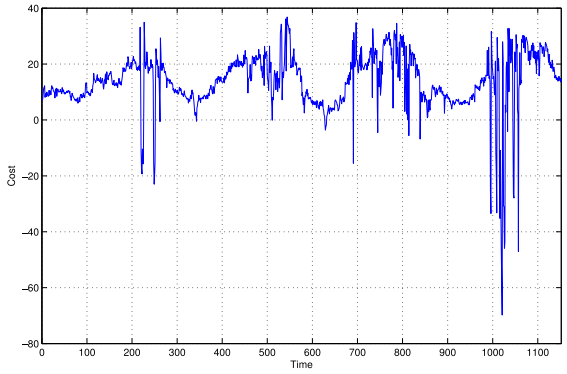

Fig. 5. Real-time cost.

C. Case Study

We apply the proposed online EMS to the microgrid using the setup described above. The voltage tolerances are set to be [0.95 and 1.05 p.u.]. The parameters in the algorithm are chosen as $\beta = 1300$, $V = 20$, $\xi_g = 1$, $\xi_b = 1$, $\xi_l = 1$, $\xi_0 = 1$, and $\xi_p = 1$. The optimization problem is solved using the CVX package [36] in MATLAB on an Intel CORE i7 3.4 GHz machine with 12 GB RAM.

Fig. 5 shows the real-time cost by using the proposed EMS. It can be seen from the figure there are some significant cost

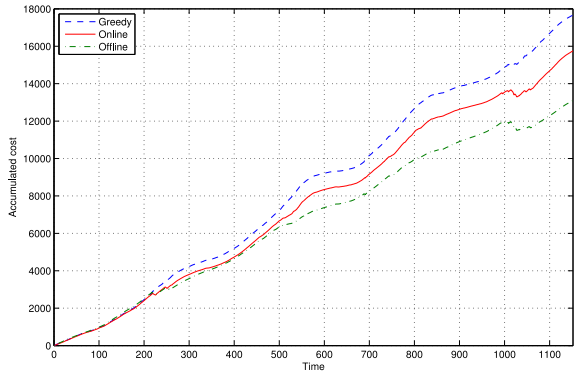

Fig. 6. Time accumulated cost comparison. Time average cost: $15.34 (greedy), $13.68 (online), and $11.37 (offline).

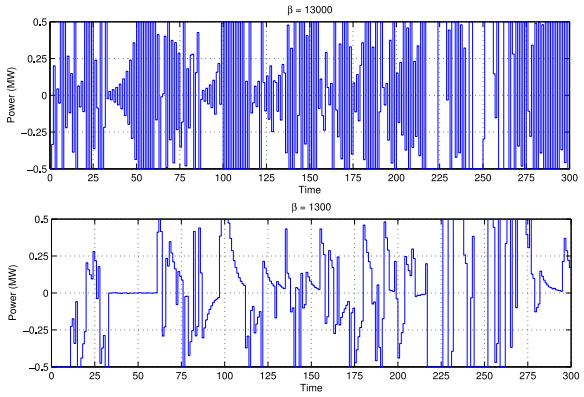

Fig. 7. Battery charging/discharging profile with different β.

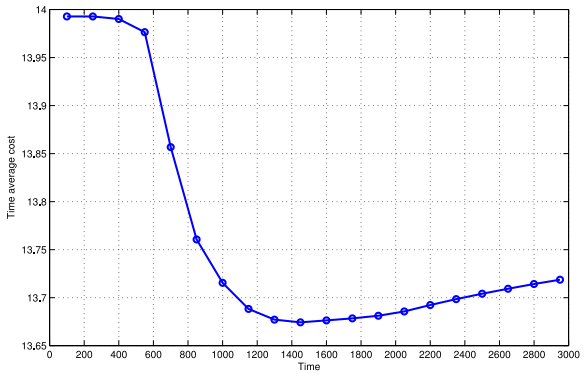

Fig. 8. Time average cost with different β.

drops, and negative costs exist, showing that the microgrid gains money by selling surplus power to the main grid at that time. If we compare Fig. 5 with Fig. 4, we can easily find that the cost drops coincide with the spikes of energy price. When the price is high, the cost of using DERs is relatively low. Therefore, it is beneficial for the microgrid not only to use DERs to supply its local demand but also to sell back surplus power to gain profit.

Next, we compare the performance of the proposed online EMS with the two benchmarks as shown by the time accumulated cost over time in Fig. 6. As shown in the figure, the shortsighted greedy algorithm performs the worst. The online EMS performs the best at first but it is surpassed by the optimal offline algorithm as time goes on. This is because the offline algorithm is optimized over the entire time horizon. It is able to make some performance sacrifices at the beginning but achieve better overall performance in the end. Although the offline algorithm gives us the best performance, it requires *a priori* system state information, which is not applicable in practice.

Regarding real-time computing, the computational time of our proposed online EMS at each time step is on average 1.13 s showing that it can be implemented in real time. The total computational time of the four-day time period (1152 time steps) is 21.65 min, compared with 3.84 h of the offline approach specified in Section IV-B. Both online and offline problems are solved using the interior-point optimizer SDPT3 [37] from CVX. Our proposed online EMS can save the computational time significantly.

For the simulations, we also verify numerically that the equality in (32) is attained in the optimal solution to OPF-r, i.e., OPF-r is an exact relaxation of OPF.

D. Discussion

1) Battery Queue: We first look at the effect of β on the charging/discharing profile of the BESS as shown in Fig. 7. As can be seen from the figure, a large β results in more charging/discharging cycles. This is because β is the weight of the battery queue stability in the optimization. A large β would push the battery queue to a less congested state and therefore cause a smaller average queue backlog. Since the battery queue backlog is the aggregate charging/discharging energy by definition, a smaller average queue backlog leads to more switches between charging (positive power) and discharging (negative power).

To investigate the effect of β on the time average cost, we run the online algorithm with different β. The result is shown in Fig. 8. The cost first drops significantly as β increases but later starts to increase once β is greater than a certain threshold. The reason for the cost drop is that the battery energy constraint is more likely to be effective when β is small and thus affects the optimality of Lyapunov optimization. After β reaches the threshold where the battery energy level can be always bounded within the required range, the time average cost increases due to the stability-and-performance tradeoff in the drift-plus-penalty function.

2) Load Queue: Fig. 9 shows the time average load shedding percentage at bus 2 with different V. From the figure, we can see that although the time average load shedding percentage may exceed the quality-of-service requirement at the beginning, it quickly converges to a point where the time average constraint (12) is satisfied as the time goes on. The figure also shows the effect of V on load shedding behaviors. As V controls the tradeoff between stabilizing queues and minimizing costs, a large V would cause the load queue to be more unstable as can be seen from Fig. 9 but incur less cost as shown in Fig. 10.

3) Voltage: In order to demonstrate the effect of the online EMS on the bus voltages of the distribution network,

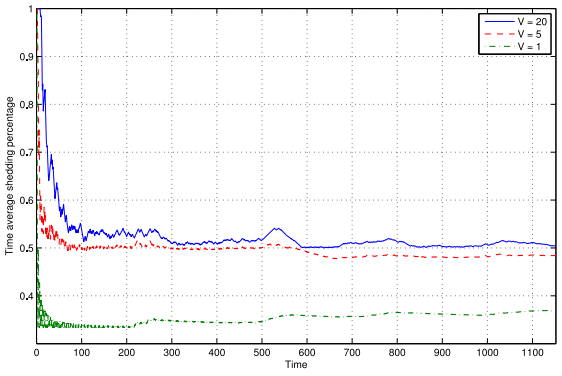

Fig. 9. Load shedding percentage at bus 2 with different V.

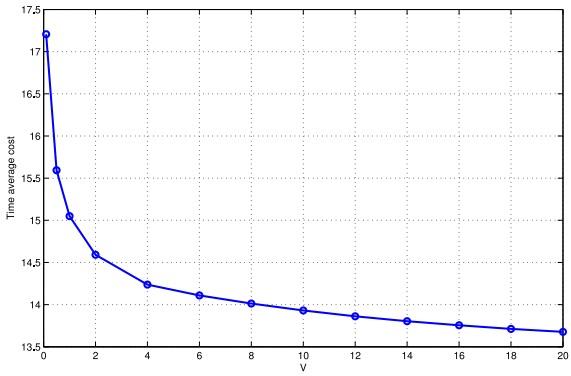

Fig. 10. Time average cost with different V.

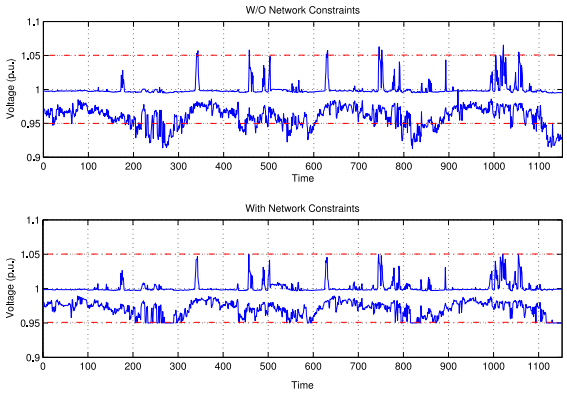

Fig. 11. Comparison of the maximum and minimum bus voltages without and with considering the network constraints (red lines indicate the allowed tolerance).

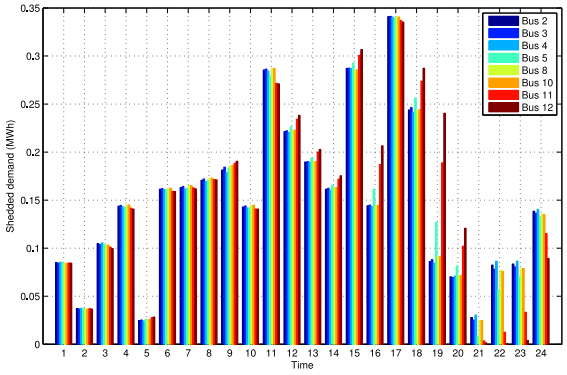

Fig. 12. Hourly shed demands at each load bus in day 3.

we conduct simulations using homogeneous loads (1.0 MW) for all load buses and increasing the line lengths by four times.

One main advantage of our proposed online EMS is that voltages in the microgrid are kept within the allowed tolerance which guarantees the power quality in the microgrid. In order to compare our proposed online EMS with the previous online algorithms [15]–[17], we also solve the microgrid energy management problem without considering the underlying network constraints and then compute the power flows in the microgrid based on the obtained control decisions. The simulated bus voltages are shown in Fig. 11. As seen from the figure, the voltages deviate significantly away from the allowed tolerance when ignoring the network constraints, which may cause serious power quality issues in the microgrid. On the contrary, our proposed online EMS can achieve the long-term objective while maintaining the voltages within the tolerance.

4) Network Effect: Another major advantage of incorporating the distribution network in the modeling is that we can now understand how the underlying network structure interacts with the online energy management. Since the loads are homogeneous, they would behave in the same way if the network constraints are not considered in the energy management as in [15]–[17]. However, the underlying network constraints have an effect on the control decisions, making the location of the bus matter in the microgrid energy management.

In order to investigate this effect, we look into the load shedding behaviors at each bus to see how they differ from each other in the online energy management. Fig. 12 shows the hourly demand reduction at each bus in day 3. It can be clearly seen from the figure that the loads at different locations behave very differently. The buses far away from the feeder and close to the DERs (e.g., buses 5, 11, and 12) are more likely to be different from the others. These buses need to shed more loads to maintain the voltage level at peak hours (e.g., hours 12–16 and 18–20) because the voltage drop along the distribution line is significant. Their demand reduction is less than the others' when the renewable generation is high (e.g., hours 11 and 21–24) because they are easier to be influenced by the injected power from the DERs. The farther the bus is away from the feeder and the closer it is to the DERs, the stronger the effect is. For example, bus 12 is influenced more than bus 11 that is more than bus 5.

V. Conclusion

An online EMS is proposed for real-time operation of microgrids in this paper. Compared with the existing online algorithms, the proposed online EMS takes into account the underlying power distribution network and the associated constraints. Specifically, we formulate the online energy management as an SOPF problem and adopt Lyapunov optimization to devise an online algorithm to solve it in real time. As one demonstration, we apply the proposed online EMS to

a real-microgrid system. The simulation results show that the performance of the proposed online EMS exceeds a greedy algorithm and is close to an optimal offline algorithm. A comprehensive analysis of the proposed online EMS is given. Through this paper, we observe and analyze the effect of the underlying network structure on the energy management that cannot be captured by previous online studies. One direction for future work is to develop an intelligent algorithm on the customer side to generate the demand requests.

Appendix A
Introduction to Lyapunov Optimization

In this paper, we develop an online EMS using Lyapunov optimization [19] which is a technique to optimize time averages in stochastic systems. We give a very brief description of it below.

Consider a stochastic system that operates in discrete time with time slots $t \in \{0, 1, 2, \ldots\}$. In every time slot, a random system state $\omega(t)$ is observed and a control action $\alpha(t)$ is taken. The control action $\alpha(t)$ is determined within a set $\mathcal{A}_{\omega(t)}$ that may depend on $\omega(t)$. There are a collection of real-valued attributes that are depended on the system state and the control action, denoted by $\mathbf{y} := (y_0(t), y_1(t), \ldots, y_L(t))$, $\mathbf{e} := (e_1(t), \ldots, e_M(t))$. Let $\bar{y}_l := \lim_{T\to\infty}(1/T)\sum_{t=0}^{T-1} y_l(t)$ and $\bar{e}_m := \lim_{T\to\infty}(1/T)\sum_{t=0}^{T-1} e_m(t)$ be the time average of $y_l(t)$ and $e_m(t)$ under a particular control. The objective is to design an algorithm that solves the following problem:

$$\min_{\{\alpha(t)\in\mathcal{A}_{\omega(t)}\}} \quad \bar{y}_0 \tag{33}$$

$$\text{s.t.} \quad \bar{y}_l \le 0, \quad l = 1, \ldots, L \tag{34}$$

$$\bar{e}_m = 0, \quad m = 1, \ldots, M. \tag{35}$$

The theory of Lyapunov optimization can be used to devise a drift-plus-penalty algorithm to solve the above problem in a simple and elegant way. The steps to use it are given briefly as follows.

1) Construct virtual queues in the way described in [19, Sec. 4.4] for ensuring that the time average constraints (34) and (35) are satisfied.
2) Define the Lyapunov function $L(t)$ as the sum of the squares of the backlogs of all the virtual queues. $L(t)$ is a scalar measurement of the queues' size.
3) Define the Lyapunov drift $\Delta(t) = L(t+1) - L(t)$ as the difference of the Lyapunov function in two consecutive time slots. It is shown in [19] that greedily minimizing the Lyapunov drift can stabilize the queues, which ensures the time average constraints are met.
4) In each time slot t, take actions to greedily minimize the drift-plus-penalty function defined as $\Delta(t) + V \times \text{penalty}(t)$, where V is a non-negative control parameter and $\text{penalty}(t)$ is a function mapped from the objective function.

The above drift-plus-penalty algorithm has been shown to produce a time average objective that deviates by at most $O(1/V)$ from the optimality with a $O(V)$ tradeoff in time average queue backlog [19].

Appendix B
Proof of Lemma 1

According to the definition of $L(\mathbf{\Theta}(t))$ in (29), we have

$$L(\mathbf{\Theta}(t+1)) - L(\mathbf{\Theta}(t)) = \frac{1}{2}\beta\sum_{b\in\mathcal{B}}\Big[J_b(t+1)^2 - J_b(t)^2\Big] + \frac{1}{2}\sum_{l\in\mathcal{L}}\Big[H_l(t+1)^2 - H_l(t)^2\Big]. \tag{36}$$

Based on the queue update of $J_b(t)$ in (25), the term $J_b(t+1)^2 - J_b(t)^2$ can upper bounded by

$$J_b(t+1)^2 - J_b(t)^2 \le 2J_b(t)p_b(t)\Delta t + \max\Big\{\underline{p}_b^2, \bar{p}_b^2\Big\}\Delta t^2. \tag{37}$$

Based on the queue update of $H_l(t)$ in (27), the term $H_l(t+1)^2 - H_l(t)^2$ can upper bounded by

$$H_l(t+1)^2 - H_l(t)^2 \le 2H_l(t)\left(\frac{\bar{p}_l(t) - p_l(t)}{\bar{p}_l(t) - \underline{p}_l(t)} - \alpha_l\right) + 1 + \alpha_l^2. \tag{38}$$

Applying (37) and (38) to (36), adding the term $V\mathbb{E}[C(t)]$, and taking the conditional expectation given $\mathbf{\Theta}(t)$ yields the upper bound in (31).

References

[1] F. Katiraei, R. Iravani, N. Hatziargyriou, and A. Dimeas, "Microgrids management," *IEEE Power Energy Mag.*, vol. 6, no. 3, pp. 54–65, May/Jun. 2008.

[2] C. Cecati, C. Citro, and P. Siano, "Combined operations of renewable energy systems and responsive demand in a smart grid," *IEEE Trans. Sustain. Energy*, vol. 2, no. 4, pp. 468–476, Oct. 2011.

[3] A. Chaouachi, R. M. Kamel, R. Andoulsi, and K. Nagasaka, "Multiobjective intelligent energy management for a microgrid," *IEEE Trans. Ind. Electron.*, vol. 60, no. 4, pp. 1688–1699, Apr. 2013.

[4] R. Palma-Behnke *et al.*, "A microgrid energy management system based on the rolling horizon strategy," *IEEE Trans. Smart Grid*, vol. 4, no. 2, pp. 996–1006, Jun. 2013.

[5] A. Khodaei, "Microgrid optimal scheduling with multi-period islanding constraints," *IEEE Trans. Power Syst.*, vol. 29, no. 3, pp. 1383–1392, May 2014.

[6] W. Shi, X. Xie, C.-C. Chu, and R. Gadh, "Distributed optimal energy management in microgrids," *IEEE Trans. Smart Grid*, vol. 6, no. 3, pp. 1137–1146, May 2015.

[7] Y. Zhang, N. Gatsis, and G. B. Giannakis, "Robust energy management for microgrids with high-penetration renewables," *IEEE Trans. Sustain. Energy*, vol. 4, no. 4, pp. 944–953, Oct. 2013.

[8] W. Su, J. Wang, and J. Roh, "Stochastic energy scheduling in microgrids with intermittent renewable energy resources," *IEEE Trans. Smart Grid*, vol. 5, no. 4, pp. 1876–1883, Jul. 2014.

[9] Z. Wang, B. Chen, J. Wang, M. Begovic, and C. Chen, "Coordinated energy management of networked microgrids in distribution systems," *IEEE Trans. Smart Grid*, vol. 6, no. 1, pp. 45–53, Jan. 2015.

[10] A. Khodaei, "Resiliency-oriented microgrid optimal scheduling," *IEEE Trans. Smart Grid*, vol. 5, no. 4, pp. 1584–1591, Jul. 2014.

[11] F. Farzan, M. A. Jafari, R. Masiello, and Y. Lu, "Toward optimal day-ahead scheduling and operation control of microgrids under uncertainty," *IEEE Trans. Smart Grid*, vol. 6, no. 2, pp. 499–507, Mar. 2015.

[12] Y. Xiang, J. Liu, and Y. Liu, "Robust energy management of microgrid with uncertain renewable generation and load," *IEEE Trans. Smart Grid*, to be published.

[13] P. Siano, C. Cecati, H. Yu, and J. Kolbusz, "Real time operation of smart grids via FCN networks and optimal power flow," *IEEE Trans. Ind. Informat.*, vol. 8, no. 4, pp. 944–952, Nov. 2012.

[14] S. Pourmousavi, M. Nehrir, C. Colson, and C. Wang, "Real-time energy management of a stand-alone hybrid wind-microturbine energy system using particle swarm optimization," *IEEE Trans. Sustain. Energy*, vol. 1, no. 3, pp. 193–201, Oct. 2010.

[15] S. Salinas, M. Li, P. Li, and Y. Fu, "Dynamic energy management for the smart grid with distributed energy resources," *IEEE Trans. Smart Grid*, vol. 4, no. 4, pp. 2139–2151, Dec. 2013.
[16] Y. Huang, S. Mao, and R. Nelms, "Adaptive electricity scheduling in microgrids," *IEEE Trans. Smart Grid*, vol. 5, no. 1, pp. 270–281, Jan. 2014.
[17] S. Sun, M. Dong, and B. Liang, "Joint supply, demand, and energy storage management towards microgrid cost minimization," in *Proc. IEEE SmartGridComm*, Venice, Italy, Nov. 2014, pp. 109–114.
[18] M. J. Neely, A. S. Tehrani, and A. G. Dimakis, "Efficient algorithms for renewable energy allocation to delay tolerant consumers," in *Proc. IEEE SmartGridComm*, Gaithersburg, MD, USA, Oct. 2010, pp. 549–554.
[19] M. J. Neely, *Stochastic Network Optimization With Application to Communication and Queueing Systems*. San Rafael, CA, USA: Morgan and Claypool, 2010.
[20] Y. Guo, M. Pan, Y. Fang, and P. P. Khargonekar, "Decentralized coordination of energy utilization for residential households in the smart grid," *IEEE Trans. Smart Grid*, vol. 4, no. 3, pp. 1341–1350, Sep. 2013.
[21] L. Zheng and L. Cai, "A distributed demand response control strategy using Lyapunov optimization," *IEEE Trans. Smart Grid*, vol. 5, no. 4, pp. 2075–2083, Jul. 2014.
[22] S. Sun, M. Dong, and B. Liang, "Real-time welfare-maximizing regulation allocation in dynamic aggregator-EVs system," *IEEE Trans. Smart Grid*, vol. 5, no. 3, pp. 1397–1409, May 2014.
[23] C. Jin, X. Sheng, and P. Ghosh, "Optimized electric vehicle charging with intermittent renewable energy sources," *IEEE J. Sel. Topics Signal Process.*, vol. 8, no. 6, pp. 1063–1072, Dec. 2014.
[24] S. Sun, M. Dong, and B. Liang, "Real-time power balancing in electric grids with distributed storage," *IEEE J. Sel. Topics Signal Process.*, vol. 8, no. 6, pp. 1167–1181, Dec. 2014.
[25] S. Lakshminarayana, T. Q. S. Quek, and H. V. Poor, "Cooperation and storage tradeoffs in power grids with renewable energy resources," *IEEE J. Sel. Areas Commun.*, vol. 32, no. 7, pp. 1386–1397, Jul. 2014.
[26] T. Li and M. Dong, "Real-time energy storage management: Finite-time horizon approach," in *Proc. IEEE SmartGridComm*, Venice, Italy, Nov. 2014, pp. 115–120.
[27] S. H. Low, "Convex relaxation of optimal power flow—Part I: Formulations and equivalence," *IEEE Trans. Control Netw. Syst.*, vol. 1, no. 1, pp. 15–27, Mar. 2014.
[28] S. H. Low, "Convex relaxation of optimal power flow—Part II: Exactness," *IEEE Trans. Control Netw. Syst.*, vol. 1, no. 2, pp. 177–189, Jun. 2014.
[29] N. Li, L. Chen, and S. H. Low, "Exact convex relaxation of OPF for radial networks using branch flow model," in *Proc. IEEE SmartGridComm*, Tainan, Taiwan, Nov. 2012, pp. 7–12.
[30] S. Sojoudi and J. Lavaei, "Physics of power networks makes hard optimization problems easy to solve," in *Proc. IEEE PES Gen. Meeting*, San Diego, CA, USA, Jul. 2012, pp. 1–8.
[31] L. Gan, N. Li, U. Topcu, and S. H. Low, "Exact convex relaxation of optimal power flow in radial networks," *IEEE Trans. Autom. Control*, vol. 60, no. 1, pp. 72–87, Jan. 2015.
[32] W. Shi, X. Xie, C.-C. Chu, and R. Gadh, "A distributed optimal energy management strategy for microgrids," in *Proc. IEEE SmartGridComm*, Venice, Italy, Nov. 2014, pp. 200–205.
[33] W. Shi, N. Li, X. Xie, C.-C. Chu, and R. Gadh, "Optimal residential demand response in distribution networks," *IEEE J. Sel. Areas Commun.*, vol. 32, no. 7, pp. 1441–1450, Jul. 2014.
[34] *National Renewable Energy Laboratory (NREL) Measurement and Instrumentation Data Center (MIDC)*. [Online]. Available: http://www.nrel.gov/midc, accessed Mar. 26, 2015.
[35] *California ISO Open Access Same-Time Information System (OASIS)*. [Online]. Available: http://oasis.caiso.com, accessed Mar. 26, 2015.
[36] M. Grant and S. Boyd. *CVX: MATLAB Software for Disciplined Convex Programming, Version 2.1*. [Online]. Available: http://cvxr.com/cvx, accessed Mar. 26, 2015.
[37] R. H. Tutuncu, K. C. Toh, and M. J. Todd, "Solving semidefinite-quadratic-linear programs using SDPT3," *Math. Program.*, vol. 95, no. 2, pp. 189–217, Feb. 2003.

Wenbo Shi (S'08) received the B.S. degree in electrical engineering from Xi'an Jiaotong University, Xi'an, China, in 2009, and the M.A.Sc. degree in electrical engineering from the University of British Columbia, Vancouver, BC, Canada, in 2011. He is currently pursuing the Ph.D. degree with the Smart Grid Energy Research Center, University of California, Los Angeles, CA, USA.

His current research interests include smart grid, such as demand response, microgrids, and energy management systems.

Na Li (M'13) received the B.S. degree in mathematics and applied mathematics from Zhejiang University, Hangzhou, China, in 2007, and the Ph.D. degree in control and dynamical systems from the California Institute of Technology, Pasadena, CA, USA, in 2013.

She is an Assistant Professor with the School of Engineering and Applied Sciences, Harvard University, Cambridge, MA, USA. She was a Postdoctoral Associate with the Laboratory for Information and Decision Systems, Massachusetts Institute of Technology, Cambridge. Her current research interests include the design, analysis, optimization, and control of distributed network systems, with particular applications to power networks and systems biology/physiology.

Ms. Li was a finalist for the Best Student Paper Award in the 2011 IEEE Conference on Decision and Control.

Chi-Cheng Chu received the B.S. degree in mechanical engineering from National Taiwan University, Taipei, Taiwan, in 1990, and the Ph.D. degree in mechanical engineering from the University of Wisconsin, Madison, WI, USA, in 2001.

He is a Project Lead with the Smart Grid Energy Research Center, University of California, Los Angeles, CA, USA. He is a Seasoned Research Manager who supervises and steers multiple industry and academia research projects in the field of smart grid, radio frequency identification technologies, mobile communication, media entertainment, 3-D/2-D visualization of scientific data, and computer aided design.

Rajit Gadh received the Bachelor's degree in mechanical engineering from the Indian Institute of Technology, Kanpur, India, in 1984; the Master's degree in mechanical engineering from Cornell University, Ithaca, NY, USA, in 1986; and the Ph.D. degree in mechanical engineering from Carnegie Mellon University, Pittsburgh, PA, USA, in 1991.

He is a Professor with the Henry Samueli School of Engineering and Applied Science, University of California, Los Angeles (UCLA), Los Angeles, CA, USA, and the Founding Director of the UCLA Smart Grid Energy Research Center. His current research interests include smart grid architectures, smart wireless communications, sense and control for demand response, microgrids and electric vehicle integration into the grid, and mobile multimedia.